Isomers of GeNO and Ge (N O) 2 : Production and infrared absorption of GeNO and ONGeNO in solid Ar

Jun-Bahn Chou, Mohammed Bahou, Yuan-Pern Lee, David Rayner, and Benoit Simard

Citation: The Journal of Chemical Physics **123**, 054321 (2005); doi: 10.1063/1.1994851
View online: http://dx.doi.org/10.1063/1.1994851
View Table of Contents: http://scitation.aip.org/content/aip/journal/jcp/123/5?ver=pdfcov
Published by the AIP Publishing

Isomers of GeNO and $Ge(NO)_2$: Production and infrared absorption of GeNO and ONGeNO in solid Ar

Jun-Bahn Chou and Mohammed Bahou
Department of Chemistry, National Tsing Hua University, 101, Section 2, Kuang Fu Road, Hsinchu 30013, Taiwan

Yuan-Pern Lee[a)]
Department of Applied Chemistry and Institute of Molecular Science, National Chiao Tung University, Hsinchu 30010, Taiwan and Institute of Molecular Sciences, Academia Sinica, Taipei 106, Taiwan

David Rayner and Benoit Simard
Steacie Institute for Molecular Sciences, National Research Council, 100 Sussex Drive, Ottawa, Canada K1A 0R6

(Received 8 April 2005; accepted 14 June 2005; published online 10 August 2005)

Crystalline germanium was ablated with light at 532 nm from a frequency-doubled neodymium: yttrium aluminum garnet laser, and the resultant plume reacted with NO before deposition onto a substrate at 13 K. Lines in group A at 1543.8 and 3059.7 cm^{-1} that become enhanced at the initial stage of irradiation at 308 or 193 nm and also after annealing are attributed to ν_1 and $2\nu_1$ of GeNO. Lines in group B at 1645.5 and 1482.8 cm^{-1} that become diminished after further irradiation of the matrix at 308 or 193 nm but become enhanced after annealing are attributed to symmetric NO stretch (ν_1) and antisymmetric NO stretch (ν_7) of ONGeNO. The assignments were derived based on wave numbers and isotopic ratios observed in the experiments with ^{15}N- and ^{18}O-isotopic substitutions and predicted with quantum-chemical calculations. Quantum-chemical calculations with density-functional theories (B3LYP and BLYP/aug-cc-pVTZ) predict four stable isomers of GeNO, six isomers of Ge_2NO, and four isomers of $Ge(NO)_2$, with linear GeNO, *cyc*-GeNGeO, and *cyc*-GeONNO having the least energies, respectively. The formation mechanisms of GeNO and ONGeNO are discussed. In addition, a weak line at 1417.0 cm^{-1} and two additional lines associated with minor matrix sites at 1423.0 and 1420.3 cm^{-1} are assigned to $GeNO^-$. © *2005 American Institute of Physics*. [DOI: 10.1063/1.1994851]

I. INTRODUCTION

Ultrathin Si oxynitride films, formed from rapid thermal oxidation of Si or SiO in a NO environment, are used as gate dielectric materials.[1] Silicon nitrosyl, SiNO, and its linear isomers NSiO and SiON have been the subject of extensive theoretical investigations.[2,3] On the investigation of the reaction of laser-ablated Si with NO molecules, three isomers SiNO, NSiO, and *cyc*-SiNO isolated in solid Ar were identified; $Si(NO)_2$ and SiNSiO were further formed upon annealing of the matrix.[4]

The greater mobility of carriers in germanium (Ge) than in silicon (Si) has promoted renewed interest in Ge-based devices for high-performance logic.[5] A key issue in the fabrication of a Ge complementary metal-oxide semiconductor (CMOS) device is to obtain a stable gate dielectric; the Ge oxynitride gate dielectric serves this purpose well. On incorporating a thin interlayer of GeO_xN_y, Chui *et al.* reported that excellent MOS capacitors with small capacitance-voltage hysteresis and small gate leakage were produced.[6] The adsorption of NO on a Ge surface[7] and transformation of NO dimers to N_2O on the Ge(100) surface have been investigated with temperature-programed desorption (TPD),[8] but little is known about the reaction of Ge atoms or its clusters with NO. It is thus of interest to investigate reactions of Ge with NO and to compare the products with those of Si with NO reported previously.[4]

Several molecular species containing one or two Ge atoms and oxygen,[9–14] sulfur,[15–17] or hydrogen[18–21] have been identified with IR or Raman spectroscopy; the spectral assignments were supported by the theoretical calculations. We reported the production of linear GeNNGe from the reaction of laser-ablated Ge with N_2 and its identification with IR-absorption spectroscopy; the unexpected activity of Ge_2 toward N_2 is supported by quantum-chemical calculations.[22] Motivated by the diversity of isomeric species that might be produced, and the importance of reactions of Ge with NO, we have undertaken experimental and theoretical investigations of $Ge_x(NO)_y$ (x and $y \leqslant 2$) with the matrix isolation technique coupled with the IR absorption spectroscopy.

II. EXPERIMENTS

The experimental setup is similar to the one described previously;[22–24] we provide only brief descriptions here. A piece of Ge (5×5 mm^2) was mounted inside the vacuum shroud of a cryogenic system about 2 cm from the target cooled to 13 K; the gaseous plume generated by laser ablation mixed with flowing reagents before deposition. Laser

[a)]Author to whom correspondence should be addressed. Electronic mail: yplee@mail.nctu.edu.tw

ablation was performed with a frequency-doubled beam from a neodymium: yttrium aluminum garnet (Nd:YAG) laser (532 nm, 30 mJ pulse^{-1}, and 10 Hz) focused onto the Ge crystal with a lens (focal length of 15 cm). Laser ablation was performed typically for 3–5 min on each spot before shifting to a new ablation position. Approximately 4–10 mmol of NO/Ar (1/100–1/800) mixture was deposited during 1–4 h.

Infrared-absorption spectra were recorded with a Fourier-transform infrared (FTIR) spectrometer (Bomem DA8) equipped with a KBr beam splitter and a Hg/Cd/Te detector (77 K) to cover the spectral range of 500–4000 cm^{-1}. Typically 300 scans at resolution of 0.5 cm^{-1} were recorded at each stage of experiment.

A XeCl excimer laser (308 nm) and an ArF excimer laser (193 nm), both operated at 5–20 Hz with energies ~10 mJ pulse^{-1}, were employed to irradiate the matrix sample to induce further photodissociation.

NO (AGA, 99.5%) was purified by passing it through a silica-gel trap maintained at 163–173 K. N ^{18}O (Cambridge Isotopes Laboratories, >90% isotopic purity) and Ar (AGA Gases, 99.995%) were used without further purification. ^{15}NO was prepared by slowly adding an aqueous solution of H_2SO_4 (10% by mass) into an aqueous solution of Na $^{15}NO_2$ (Isotec, 99% isotopic purity);[25] the gas thus produced was passed through a solution of KOH to trap the HNO_3 byproduct, and the collected gas was further purified by passing it through a silica-gel trap maintained at 163–173 K. Solid Ge was cut from a Ge crystal employed previously in attenuated-total-reflection (ATR) experiments.

III. COMPUTATIONAL METHOD

The equilibrium structures, vibrational frequencies, IR intensities, and energies were calculated with GAUSSIAN03 program.[26] Our calculations are based on BLYP and B3LYP density-functional theories (DFT); the latter method uses Becke's three-parameter hybrid exchange functional,[27] which includes the Slater exchange functional with corrections involving a gradient of the density, and a correlation functional of Lee *et al.* with both local and nonlocal terms.[28] Dunning's correlation-consistent polarized valence triple-zeta[29] (aug-cc-pVTZ) basis set augmented with *s*, *p*, *d*, and *f* functions was used. Analytic first and second derivatives were applied for geometry optimization and vibrational frequencies at each stationary point.

IV. EXPERIMENTAL RESULTS

A. Reactions of Ge with NO

The IR spectrum of a sample of NO/Ar (1/200) at 13 K exhibits multiple lines due to NO (1871.8 cm^{-1}) and *cis*-$(NO)_2$ (3608.7, 1863.4, and 1776.4 cm^{-1}),[30] and weak lines due to *trans*-$(NO)_2$ (1747.2 cm^{-1})[30] and NO_2 (2902.2 and 1610.9 cm^{-1}). A partial spectrum of the matrix sample is shown in trace (A) of Fig. 1. The IR spectrum of a sample deposited at 13 K from the reaction of a plume from laser-ablated Ge with a flowing gaseous mixture of NO/Ar (1/100) exhibits additional weak multiple lines due to *cis*-$(NO)_2^-$ at 2492.0, 1300.4, 1222.9, and 884.4 cm^{-1},[31]

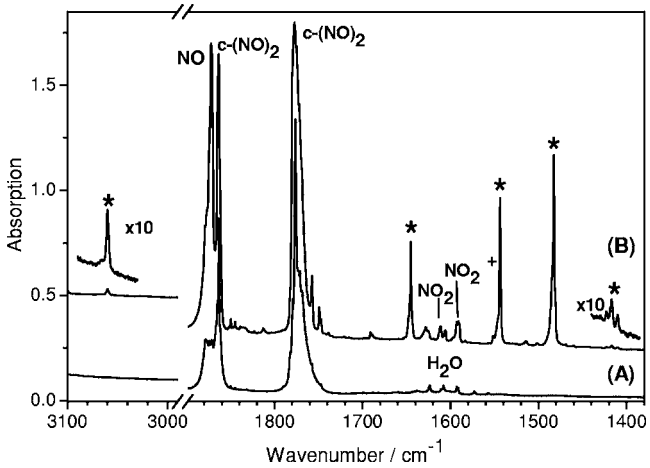

FIG. 1. Partial IR spectra of (A) a NO/Ar (1/200) matrix and (B) a matrix codeposited with NO/Ar (1/100) and laser-ablated Ge in regions of 1380–1900 and 2990–3100 cm^{-1}. New lines are marked with *.

trans-$(NO)_2^-$ at 1221.0 cm^{-1},[31] NO_2^- at 1243.6 cm^{-1},[32] $(NO)_2^+$ at 1589.4 and 1583.4 cm^{-1},[31] N_2O at 2218.5 cm^{-1}, GeO at 971.3 cm^{-1},[9] and new lines at 1417.0, 1482.8, 1543.8, 1645.5, and 3059.7 cm^{-1}, as indicated with * in trace (B) of Fig. 1. These new lines are separated into three groups according to their behavior upon laser irradiation and annealing. The lines in group A at 1543.8 (1546.7, 1552.0) and 3059.7 cm^{-1} increase at the initial stage of irradiation at 308 and 193 nm and also upon annealing, but decrease at a subsequent stage of irradiation; the lines listed in parentheses are associated with the species in minor matrix sites. The lines in group B at 1645.5 and 1482.8 cm^{-1} diminish nearly completely upon irradiation of the matrix sample at 308 nm, diminish to a lesser extent upon irradiation at 193 nm, but increase in intensity upon annealing. The extremely weak lines in group C at 1417.0 (1423.0, 1420.1) cm^{-1} diminish upon laser irradiation at 308 and 193 nm, and upon annealing; the lines listed in parentheses are associated with the species in minor matrix sites. As the concentration of the NO/Ar mixture is decreased from 1/100 to 1/800, the intensity of group B decreases to a tenth of that of group A, whereas the intensity of group C increases slightly.

B. Reaction of Ge with a mixture of ^{14}NO and ^{15}NO

When a mixture containing Ar and isotopically labeled ^{14}NO and ^{15}NO in a proportion of ~1:0.9 was codeposited with laser-ablated Ge, the line due to NO at 1871.8 cm^{-1} splits into two lines with an additional line at 1838.9 cm^{-1}, and each line of *cis*-$(NO)_2$ at 1776.4 and 1863.4 cm^{-1} splits into a triplet, with additional lines at 1757.8, 1744.8, 1849.7, and 1830.6 cm^{-1}.[30]

Each line in group A, at 1543.8 (1546.7, 1552.0) and 3059.7 cm^{-1}, splits into two lines with additional lines at 1513.7 (1516.5, 1521.8) and 3000.9 cm^{-1}, as listed in Table I; the lines in the region of 1370–1660 cm^{-1} are depicted in Fig. 2(b). These doublets display similar patterns with relative integrated intensities nearly the same as the proportion

TABLE I. Vibrational wave numbers (cm^{-1}) of new lines observed in the experiments on codeposition of laser-ablated Ge with a mixture of NO/Ar (1/100). The wave numbers associated with minor sites are listed in parentheses.

Group A	NO stretch (ν_1)	Overtone ($2\nu_1$)
$Ge^{14}N^{16}O$	1543.8 (1546.7, 1552.0)	3059.7
$Ge^{15}N^{16}O$	1513.7 (1516.5, 1521.8)	3000.9
$Ge^{14}N^{18}O$	1509.8 (1512.5, 1517.6)	2993.5
Group B	**Symmetric-NO stretch (ν_1)**	**Antisymmetric-NO stretch (ν_7)**
$^{16}O^{14}NGe^{14}N^{16}O$	1645.5	1482.8
$^{16}O^{14}NGe^{15}N^{16}O$	1631.5	1469.1
$^{16}O^{15}NGe^{15}N^{16}O$	1615.5	1457.7
$^{16}O^{14}NGe^{14}N^{18}O$	1627.0	1460.3
$^{18}O^{14}NGe^{14}N^{18}O$	1603.9	1443.0
Group C	**Symmetric-NO stretch (ν_1)**	
$Ge^{14}N^{16}O^-$	1417.0 (1420.1, 1423.0)	
$Ge^{15}N^{16}O^-$	1386.9 (1389.7, 1393.3)	
$Ge^{14}N^{18}O^-$	1390.3 (1392.7, 1395.5)	

of ^{14}NO and ^{15}NO employed in this experiment. Our observation of only doublets for the lines of group A in the experiments with mixed ^{14}N and ^{15}N isotopes indicates that only one N atom is involved in these vibrational modes. The ^{15}N-isotopic ratios, defined as the ratio of vibrational wave number of species containing ^{15}N to that containing ^{14}N, 0.9804 and 0.9807 for the lines at 1543.8 and 3059.7 cm^{-1}, respectively, are similar to but slightly smaller than the theoretical ^{15}N-isotopic ratio of 0.9824 for NO.

Each line in group B, at 1645.5 and 1482.8 cm^{-1}, splits into three lines with additional lines at (1631.5, 1615.5) and (1469.1, 1457.7) cm^{-1}, as listed in Table I and illustrated in Fig. 2(b). These triplets display similar patterns with relative integrated intensities ~1.0:1.8:0.8; this pattern indicates that two equivalent N atoms are involved in these vibrational modes. The ^{15}N-isotopic ratios of 0.9817 and 0.9830 for the lines at 1645.5 and 1482.8 cm^{-1}, respectively, are similar to the theoretical ^{15}N-isotopic ratio of 0.9824 for NO. The wave numbers of these two modes indicate that these lines might be associated with symmetric and antisymmetric N–O stretching modes.

Each line in group C at 1417.0 (1420.1, 1423.0) cm^{-1} splits into two lines with the additional line at 1386.9 (1389.7, 1393.3) cm^{-1}, as shown in Table I and in Fig. 2(b). The relative intensities of these doublets indicate that only one N atom is involved in this vibrational mode. The ^{15}N-isotopic ratio of 0.9787 is slightly smaller than the theoretical ^{15}N-isotopic ratio of 0.9824 for NO.

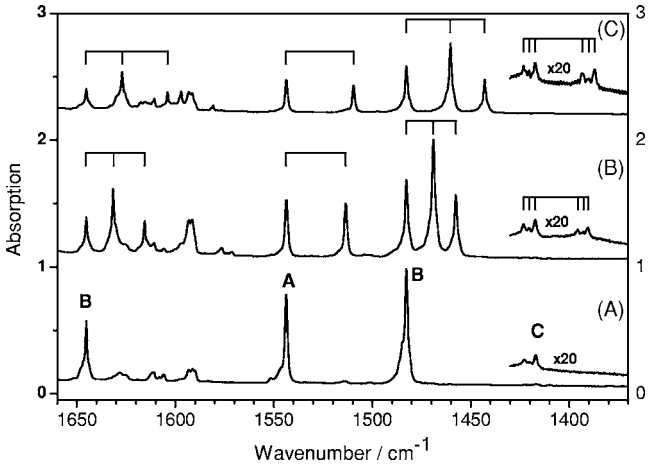

FIG. 2. Isotopic-substitution spectra of new lines in the region of 1370–1660 cm^{-1}. (A) codeposition of laser-ablated Ge and NO/Ar (1/100) in natural abundance, (B) codeposition of laser-ablated Ge and a mixture of $^{14}NO/^{15}NO/Ar$ (1/0.9/200), and (C) codeposition of laser-ablated Ge and a mixture of $N\ ^{16}O/N^{18}O/Ar$ (1/0.85/200). The lines associated with groups A–C are labeled.

C. Reaction of Ge with a mixture of $N\ ^{16}O$ and $N\ ^{18}O$

When a mixture of $N\ ^{16}O$ and $N\ ^{18}O$ (diluted in Ar) in a proportion of ~1:0.85 was codeposited with laser-ablated Ge, the line due to NO at 1871.8 cm^{-1} splits into two lines with an additional line at 1823.4 cm^{-1}, and each line of *cis*-$(NO)_2$ at 1776.4 and 1863.4 cm^{-1} each splits into a triplet, with additional lines at 1747.2, 1730.2, 1845.0, and 1815.1 cm^{-1}.

Each line in group A, at 1543.8 (1546.7, 1552.0), and 3059.7 cm^{-1}, splits into two lines with additional lines at 1509.8 (1512.5, 1517.6) and 2993.5 cm^{-1}, as listed in Table I; the lines in the region of 1370–1660 cm^{-1} are illustrated in Fig. 2(c). These doublets display similar patterns with relative integrated intensities nearly the same as the proportion of $N\ ^{16}O$ and $N\ ^{18}O$ employed in this experiment. Our observation of only doublets for the lines in group A in the experiments with mixed ^{16}O and ^{18}O isotopes indicates that only one O atom is involved in these vibrational modes. The ^{18}O-isotopic ratios, 0.9780 and 0.9783 for the lines at 1543.8 and 3059.7 cm^{-1}, respectively, are similar to but slightly greater than the theoretical ^{18}O-isotopic ratio of 0.9741 for NO.

Each line in group B, at 1645.5 and 1482.8 cm^{-1}, splits into three lines with additional lines at (1627.0, 1603.9) and (1460.3, 1443.0) cm^{-1}, as listed in Table I and illustrated in Fig. 2(c). These triplets display similar patterns with relative integrated intensities ~1.0:1.7:0.7; this pattern indicates that two equivalent O atoms are involved in these vibrational modes. The ^{18}O-isotopic ratios are 0.9747 and 0.9731 for the lines at 1645.5 and 1482.8 cm^{-1}, respectively, similar to the theoretical ^{18}O-isotopic ratio of 0.9741 for NO.

Each line in group C at 1417.0 (1420.1, 1423.0) cm^{-1} splits into two lines with the additional line at 1390.3 (1392.7, 1395.5) cm^{-1}, as listed in Table I and illustrated in Fig. 2(c). This doublet pattern indicates that only one O atom is involved in this vibrational mode. The ^{18}O-isotopic ratio of 0.9811 is greater than the theoretical ^{18}O-isotopic ratio of 0.9741 for NO.

In summary, the lines in groups A and C are associated with the species containing one NO, whereas the lines in group B are associated with the species containing two equivalent NO groups. The observed relative intensities in NO-dilution experiments and annealing experiments also support such assignments.

TABLE II. Relative energies and geometries of four isomers and four ions of GeNO predicted with BLYP/aug-cc-pVTZ.

Species	Energy[a] (kJ mol^{-1})	R(GeN) (Å)	R(GeO) (Å)	R(NO) (Å)
GeNO	0	1.785		1.212
cyc-GeNO[b]	42.5	1.898	1.939	
NGeO	135.4	1.755	1.657	
GeON	136.7		1.846	1.243
$GeNO^+$	773.7	1.905		1.168
$GeNO^-$	−177.1	1.749		1.253
$GeON^+$	851.0		1.899	1.214
$GeON^-$	11.3		1.846	1.253

[a]Energies relative to that calculated for linear GeNO, −2207.048 522 hartree with BLYP/aug-cc-pVTZ; the listed energies are corrected with zero-point energies.
[b]∠NGeO=42.8°.

V. QUANTUM-CHEMICAL CALCULATIONS

A. Isomers and ions of GeNO and Ge_2NO

With the theoretical calculations according to the B3LYP and BLYP density-functional theories using aug-cc-pVTZ basis sets, we located four isomers of GeNO. For brevity, we only list the results from BLYP here and compare the results of BLYP and B3LYP in Electronic Physics Auxiliary Publication Service (EPAPS).[33] Table II lists the geometries and relative energies of these isomers. Our previous quantum-chemical calculations on isomers of N_2O_3 indicate that, for systems containing more than one NO group, BLYP predicts vibrational wave numbers better than B3LYP.[34] According to the calculations with BLYP/aug-cc-pVTZ, linear GeNO has the least energy; the N–O bond length is 1.212 Å, slightly greater than that of NO (1.151 Å).[35] The calculated Ge–N bond length of 1.785 Å is slightly greater than that for diatomic GeN (1.669 Å) predicted with the calculations at the same level. A cyclic isomer *cyc*-GeNO has an energy about 42.5 kJ mol^{-1} above that of linear GeNO; it has a N–O bond length of 1.401 Å and a Ge–N bond length of 1.898 Å, both greater than those calculated for GeNO. The other two linear isomers, NGeO and GeON, both lie ~136 kJ mol^{-1} above linear GeNO.

Because ions might be formed during laser ablation, we also calculated positive and negative ions of these species; only the results for ions of GeNO and GeON are listed in Table II for comparison. $GeNO^-$ lies ~177 kJ mol^{-1} below GeNO, whereas $GeNO^+$ lies 774 kJ mol^{-1} above GeNO. The stabilization energy of $GeON^-$ relative to GeON is ~125 kJ mol^{-1}. The length of the N–O bond increases from 1.212 to 1.253 Å from GeNO to $GeNO^-$, whereas the length of the Ge–N bond decreases from 1.785 to 1.749 Å. In contrast, $GeNO^+$ shows an opposite trend with an elongated Ge–N bond and a shorter N–O bond, as compared with GeNO.

Vibrational wave numbers and IR intensities for each isomer, calculated with BLYP/aug-cc-pVTZ are listed in Table III. Because the observed feature in the N–O stretching region is 1543.8 cm^{-1} for group A and 1417.0 cm^{-1} for group C, we expect that the calculated vibrational wave numbers corresponding to this mode fall within a range of 1200–1700 cm^{-1}.

TABLE III. Vibrational wave numbers (σ) and IR intensities of four isomers and four ions of GeNO predicted with BLYP/aug-cc-pVTZ.

			BLYP	
Species	ν_i	Mode	σ (cm^{-1})	IR intensity (km mol^{-1})
GeNO	ν_1	NO stretch	1531.4	417
	ν_2	GeN stretch	522.0	15.6
	ν_3	Bend	298.6	19.3
	ν_4	Bend	240.0	3.8
cyc-GeNO	ν_1	NO stretch	931.6	70.9
	ν_2	GeN stretch	592.5	17.7
	ν_3	GeO stretch	353.7	2.7
NGeO	ν_1	GeO stretch	907.4	16.9
	ν_2	GeN stretch	739.0	3.7
	ν_3	Bend	156.7	17.7
	ν_4	Bend	137.2	27.1
GeON	ν_1	NO stretch	1211.6	237
	ν_2	GeO stretch	384.3	0.1
	ν_3	Bend	262.8	8.3
	ν_4	Bend	217.5	2.1
$GeNO^+$	ν_1	NO stretch	1693.8	279
	ν_2	GeO stretch	402.7	9.4
	ν_3	Bend	190.7	2.0
$GeNO^-$	ν_1	NO stretch	1402.6	889
	ν_2	GeO stretch	554.8	23.9
	ν_3	Bend	322.2	49.6
$GeON^+$	ν_1	NO stretch	1242.2	192
	ν_2	GeO stretch	327.1	0.1
	ν_3	Bend	198.5	3.8
$GeON^-$	ν_1	NO stretch	1254.6	638
	ν_2	GeO stretch	406.1	0.2
	ν_3	Bend	315.3	25.5

For the line at 1543.8 cm^{-1} the best fit is the N–O stretching (ν_1) mode of linear GeNO; the predicted vibrational wave number is 1531 cm^{-1} with an IR intensity of 417 km mol^{-1} using the BLYP method. The other vibrational wave numbers predicted for these four neutral isomers have vibrational wave numbers below 1250 cm^{-1}. The ions of GeNO also have vibrational wave numbers, 1694 cm^{-1} for $GeNO^+$ and 1403 cm^{-1} for $GeNO^-$ (1765 and 1478 cm^{-1}, respectively, from B3LYP), near the experimental value, but the ~10% deviations are greater than that expected for the calculations using the aug-cc-pVTZ basis sets.

For the line at 1417.0 cm^{-1} in group C, the best fit is the N–O stretching (ν_1) mode of linear $GeNO^-$; predicted to be 1403 cm^{-1} with an IR intensity of 889 km mol^{-1} using the BLYP method. Other possible candidates are GeON (1255 cm^{-1}), $GeON^+$ (1242 cm^{-1}), and GeNO (1531 cm^{-1}), but they have deviations of 9%–12%.

We also located six isomers of Ge_2NO with quantum-chemical calculations. Geometries, relative energies, vibrational wave numbers, and IR intensities of these isomers may be found in EPAPS.[33] The only candidate that has a predicted vibrational wave number close to that of observed lines is *cyc*-(GeGeN)=O which has ν_1=1356 cm^{-1} (from BLYP), similar to that of the observed line of group C at 1417.0 cm^{-1}.

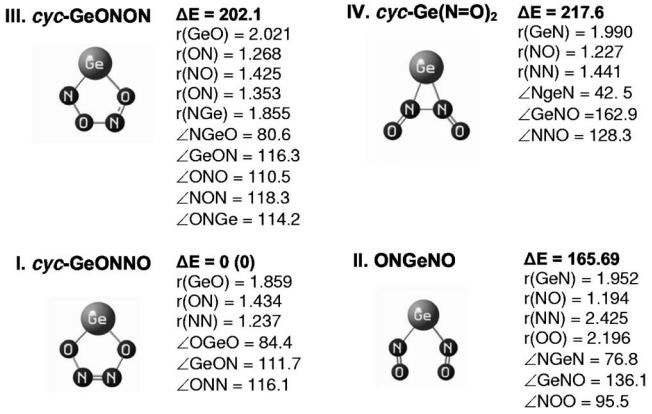

FIG. 3. Structures and relative energies of four isomers of $Ge_2(NO)_2$ calculated with BLYP/aug-cc-pVTZ. Bond lengths are in Å, bond angles in degrees, and relative energies in kJ mol^{-1}.

B. Isomers of $Ge(NO)_2$

We located four stable isomers of $Ge(NO)_2$. Figure 3 depicts the geometries and relative energies of these isomers. According to the BLYP/aug-cc-pVTZ calculations, *cyc*-GeONNO has the least energy; the N–O bond length is 1.434 Å, much greater than that of NO (1.151 Å).[35] The calculated N–N bond length of 1.237 Å is shorter than that of *cis*-$(NO)_2$ (2.081 Å) and only slightly greater than that of N_2O (1.121 Å) predicted with the calculations at the same level. An open-chain isomer ONGeNO has an energy about 166 kJ mol^{-1} above *cyc*-GeONNO; it has a N–O bond length of 1.194 Å similar to that (1.212 Å) of GeNO, whereas its Ge–N bond length (1.952 Å) is greater than that (1.785 Å) of GeNO. The third isomer, *cyc*-GeONON, is predicted to have an energy of ~202 kJ mol^{-1} above *cyc*-GeONNO; all the three NO bond lengths predicted (1.268, 1.425, and 1.353 Å) are greater than that of NO; the two NO moieties are inequivalent. *cyc*-$Ge(N{=}O)_2$ lies ~218 kJ mol^{-1} above *cyc*-GeONNO; it has NO bonds and GeN bonds slightly longer than those of its open-form counterpart, ONGeNO. Relative energies calculated with B3LYP are greater and with different ordering for other isomers of $Ge(NO)_2$, as shown in EPAPS.[33]

The predicted vibrational wave numbers and IR intensities for each isomer are listed in Table IV. Because the observed features of group B are at 1645.5 and 1482.8 cm^{-1}, we expect that the calculated vibrational wave numbers corresponding to these modes fall within a range 1250–1850 cm^{-1}. The best fit is the symmetric (ν_1) and the antisymmetric N–O stretching (ν_7) mode of ONGeNO; the predicted vibrational wave numbers are 1628.6 and 1476.8 cm^{-1} with respective IR intensities of 225 and 607 km mol^{-1} using the BLYP method. The observed relative intensity of ~1:3 for these two lines is also consistent with the predicted IR intensities. The other three isomers have no modes with vibrational wave numbers and relative intensities similar to our experimental observations. The only possible alternative candidate is *cyc*-$Ge(NO)_2$, with vibrational wave numbers of two N–O stretching modes predicted at 1438.5 and 1439.1 cm^{-1} (1494.2 and 1525.6 cm^{-1} from B3LYP); the predicted intensities of these two lines are approximately equal.

VI. DISCUSSION

Because the observed absorption lines are associated with the N–O stretching modes, variations in mass of Ge have little effect on these vibrational wave numbers. In the calculation that we performed on ^{70}GeNO and ^{76}GeNO, we found that the variation in vibrational wave number of the N–O stretching mode was only 0.1 cm^{-1}, too small to be resolved under our experimental conditions. Hence, isotopic ratios for only ^{15}N and ^{18}O species are calculated and compared with the experimental observations, as listed in Tables V and VI.

A. Assignments of lines in group A to GeNO

Observed ^{15}N- and ^{18}O-isotopic patterns indicate that the feature near 1543.8 cm^{-1} in group A is associated with a vibrational mode involving the N–O stretch. The observation of a ^{15}N-isotopic ratio slightly smaller and an ^{18}O-isotopic ratio slightly greater than those of diatomic NO indicates that Ge is attached to the N atom rather than the O atom so that the effective mass of N in the N–O stretching mode is increased. The assignment of this line to GeNO is consistent with the comparison of observed and predicted vibrational wave numbers, as discussed in Sec. V. We calculated the vibrational wave numbers of ^{15}N-substituted and ^{18}O-substituted species of all four isomers of GeNO and ions of GeNO and GeON. The predicted isotopic ratios, defined as the ratio of vibrational wave number of the isotopically substituted species to that of the corresponding species containing ^{74}Ge, ^{14}N, and ^{16}O, for the N–O stretching mode, are listed in Table V; the experimental values are listed at the top for comparison.

Similar to the vibrational wave numbers of the N–O stretching mode, the predicted isotopic ratios of GeNO in all isotopic variants show the best agreement with the experiments for the line at 1543.8 cm^{-1}, with deviations of 0.0002 for the ^{15}N ratio and 0.0008 for the ^{18}O ratio calculated with BLYP/aug-cc-pVTZ. Other isomers have calculated isotopic ratios deviating from the experiments much greater than those for GeNO. Although we cannot positively exclude $GeNO^-$ and *cyc*-$(GeGeN){=}O$, for both of which have isotopic ratios deviate less than 0.0032, as possible carriers of the line at 1543.8 cm^{-1}, the ~10% deviations between predicted wave numbers and experimental observations are much greater than one would expect for quantum-chemical calculations using the BLYP/cc-pVTZ method.

Although a definitive proof of the assignment should come from direct observation of the Ge–N stretching mode near 545 cm^{-1}, we fail to observe this line because of the small intensity (less than 4% of the N–O stretching mode predicted with theory) and the much worse detectivity in this region. We *assign the feature at* 1543.8 cm^{-1} to the N–O stretching mode of GeNO based both on the agreement of vibrational wave numbers and isotopic ratios between observation and those predicted for GeNO and on the fact that GeNO is the isomer with the least energy and is the expected product of the reaction of Ge+NO.

The line at 3059.7 cm^{-1} shows similar isotopic ratios and has a wave number nearly twice that of the line at

TABLE IV. Relative energies, vibrational wave numbers (σ), and IR intensities of four isomers of $Ge(NO)_2$ predicted with BLYP/aug-cc-pVTZ.

				BLYP	
Energy[a] (kcal mol^{-1})	ν_i	Vibrational symmetry	Mode	σ (cm^{-1})	IR intensity (km mol^{-1})
I. *cyc*-GeONNO					
0	ν_1	A_1	N═N stretch	1418.0	27
	ν_2	A_1	*s*-NO stretch	733.0	75
	ν_3	A_1	*s*-GeO stretch	639.6	2.9
	ν_4	A_1	OGeO bend	401.5	34
	ν_5	A_2	Out-of-plane deformation	598.1	0.0
	ν_6	B_1	Out-of-plane deformation	296.6	5.6
	ν_7	B_2	ONN bend	896.5	5.2
	ν_8	B_2	*a*-NO stretch	641.8	89
	ν_9	B_2	*a*-GeO stretch	415.6	3.8
II. ONGeNO					
165.7	ν_1	A_1	*s*-NO stretch	1628.6	225
	ν_2	A_1	*s*-GeN stretch	514.5	3.6
	ν_3	A_1	NGeN bend	357.1	38
	ν_4	A_1	*s*-GeNO bend	283.9	0.0
	ν_5	A_2	Out-of-plane deformation	396.1	0.0
	ν_6	B_1	Out-of-plane deformation	354.1	8.9
	ν_7	B_2	*a*-NO stretch	1476.8	607
	ν_8	B_2	*a*-GeNO bend	570.3	0.4
	ν_9	B_2	*a*-GeN stretch	216.8	8.2
III. *cyc*-GeONON					
202.1	ν_1	A'	NO stretch	1182.6	89.7
	ν_2	A'	Mixed	969.1	60.7
	ν_3	A'	ONO bend	872.9	16.4
	ν_4	A'	GeN stretch	647.5	18.6
	ν_5	A'	GeON bend	449.2	14.4
	ν_6	A'	ON stretch	400.0	2.4
	ν_7	A'	In-plane deformation	261.4	7.5
	ν_8	A''	Out-of-plane deformation	557.2	0.01
	ν_9	A''	Out-of-plane deformation	333.8	8.5
IV. *cyc*-Ge(N═O)$_2$					
217.6	ν_1	A_1	*s*-NO stretch	1439.1	405
(244.3)	ν_2	A_1	N–N stretch	623.9	29
	ν_3	A_1	*s*-GeN stretch	425.3	4.7
	ν_4	A_1	*s*-ONN bend	208.2	15
	ν_5	A_2	Out-of-plane deformation	527.9	0.0
	ν_6	B_1	Out-of-plane deformation	240.1	0.0
	ν_7	B_2	*a*-NO stretch	1438.5	409
	ν_8	B_2	*a*-ONN bend	849.3	6.0
	ν_9	B_2	GeNN bend	254.0	0.7

[a]Energies relative to that calculated for *cyc*-GeONNO, −2337.080 535 hartree, with BLYP/aug-cc-pVTZ. All energies are corrected with zero-point energies.

1543.8 cm^{-1}. It is hence assigned as the first overtone of the NO stretching mode of GeNO. The anharmonicity $\omega_e x_e$ is consequently determined to be 14.0 cm^{-1}.

B. Assignments of lines in group B to ONGeNO

The observed ^{15}N- and ^{18}O-isotopic patterns indicate that the features near 1645.5 and 1482.8 cm^{-1} in group B are associated with the vibrational modes involving stretching of N–O bonds; these lines are likely associated with the symmetric and antisymmetric N–O stretching modes. We calculated the isotopic ratios for the ^{15}N-substitued and ^{18}O-substitutes species for all vibrational modes of all three isomers of $Ge(NO)_2$ that have equivalent NO moieties, but we list in Table VI only those of symmetric and antisymmetric N–O stretching modes to compare with the experiments. The predicted isotopic ratios of ONGeNO in all ^{15}N- and ^{18}O-isotopic variants show the best agreement with the experiments, with deviations less than 0.0003 for the ^{15}N ratio and less than 0.0005 for the ^{18}O ratio calculated with BLYP/aug-cc-pVTZ. The other candidate that has predicted wave numbers barely within the range of expected uncertainties, *cyc*-Ge(N═O)$_2$, has isotopic ratios calculated with BLYP and B3LYP that deviate by as much as 0.0116 and 0.0059, respectively.

TABLE V. Comparison of observed isotopic ratios [ratios of ν(isotopomer)/$\nu(^{74}Ge^{14}N^{16}O)$] for lines in groups A and C (listed in italic) with those predicted for the N–O stretching mode of isomers and ions of GeNO with BLYP/aug-cc-pVTZ.

Expt.	^{15}N ratio	^{18}O ratio
(*A*) *1543.8 cm^{-1}*	*0.9804*	*0.9780*
3059.7 cm^{-1}	*0.9807*	*0.9783*
(*C*) *1417.0 cm^{-1}*	*0.9787*	*0.9811*
Calculations		
Linear GeNO	0.9802	0.9772
cyc-GeNO	0.9852	0.9706
Linear GeON	0.9818	0.9744
cyc-(GeGeN)═O	0.9816	0.9748
trans-GeNOGe	0.9728	0.9915
cis-GeNOGe	0.9774	0.9829
Linear $GeNO^-$	0.9785	0.9802
Linear $GeNO^+$	0.9818	0.9743
Linear $GeON^-$	0.9826	0.9729
Linear $GeON^+$	0.9797	0.9780

Although a definitive proof of the assignment should come from direct observation of the symmetric Ge–N stretching mode near 524 cm^{-1}, we fail to observe this line because of the small intensity (less than 2% of the symmetric N–O stretching mode predicted with theory) and the much worse detectivity in this region. Based on the excellent agreement of the vibrational wave numbers and isotopic ratios between observations and predictions for ONGeNO and the enhanced intensities of these features when a greater concentration of NO was employed, we *deduce* that features in group B at 1645.5 and 1482.8 cm^{-1} correspond to the symmetric and antisymmetric N═O stretching modes of ONGeNO.

C. Assignments of lines in group C to $GeNO^-$

The observed ^{15}N- and ^{18}O-isotopic patterns indicate that the extremely weak feature near 1417.0 cm^{-1} in group C is associated with a vibrational motion involving stretching of a N–O bond. From the calculated isotopic ratios listed in Table V, the predicted values of $GeNO^-$ show the best agreement with the experiments, with deviations of 0.0002 for the ^{15}N ratio and 0.0009 for the ^{18}O ratio calculated with BLYP/aug-cc-pVTZ. The next best fit is *cis*-GeNOGe, with deviations of 0.0013 for the ^{15}N ratio and 0.0018 for the ^{18}O ratio. Other isomers have calculated isotopic ratios deviating by greater than 0.003 for the ^{15}N ratio and 0.006 for the ^{18}O ratio. Although we cannot positively exclude *cis*-GeNOGe as a possible carrier of this line at 1417.0 cm^{-1}, the ~16% deviations between predicted wave numbers and experimental observation are much greater than one would expect for quantum-chemical calculations using the BLYP/cc-pVTZ method.

Similarly, although the predicted vibrational wave number of *cyc*-(GeGeN)═O is only 4.7% smaller than that of the feature at 1417.0 cm^{-1}; its ^{15}N- and ^{18}O-isotopic ratios deviate from the experiments by 0.0029 and 0.0063, much greater than the expected maximum uncertainty of 0.003. We thus assign the *weak feature* at 1417.0 cm^{-1} to the N–O stretching mode of $GeNO^-$ based on the agreement of the vibrational wave numbers and isotopic ratios between observation and prediction. The enhanced intensity of this feature relative to that of GeNO upon dilution of NO in Ar is also consistent with the behavior expected for ion production.

TABLE VI. Comparison of observed isotopic ratios [ratios of ν(isotopomer)/$\nu(^{74}Ge^{14}N^{16}O)$] for lines in group B (listed in italic) with those predicted for the N–O stretching mode of symmetric isomers of $Ge(NO)_2$ with BLYP/aug-cc-pVTZ.

Symmetric-NO stretch	$^{14}N,^{15}N$ species	$^{15}N,^{15}N$ species	$^{16}O,^{18}O$ species	$^{18}O,^{18}O$ species
Expt. (*1645.5 cm^{-1}*)	*0.9914*	*0.9817*	*0.9887*	*0.9747*
Calc.				
ONGeNO	0.9917	0.9818	0.9888	0.9742
cyc-GeONNO	0.9922	0.9846	0.9858	0.9712
cyc-Ge(N—O)$_2$	0.9998	0.9820	0.9998	0.9742
Asymmetric-NO stretch	$^{14}N,^{15}N$ species	$^{15}N,^{15}N$ species	$^{16}O,^{18}O$ species	$^{18}O,^{18}O$ species
Expt. (*1482.8 cm^{-1}*)	*0.9907*	*0.9830*	*0.9848*	*0.9731*
Calc.				
ONGeNO	0.9906	0.9828	0.9844	0.9726
cyc-GeONNO	0.9902	0.9849	0.9974	0.9704
cyc-Ge(N—O)$_2$	0.9805	0.9788	0.9771	0.9796

D. Mechanism of formation

The formation of GeNO from the reaction of laser-ablated Ge with NO upon deposition and upon annealing is consistent with our previous experience that typically the isomer of the least energy is produced. The bonding energy of Ge–NO is about 230 kJ mol^{-1}. We sought for GeON, *cyc*-GeNO, and NGeO but found no absorption line ascribable to these species even though our theoretical calculations indicate that isomerization from GeNO to *cyc*-GeNO and to GeON is energetically accessible.

The formation of ONGeNO might proceed via insertion of Ge into *cis*-$(NO)_2$,

$$\mathrm{Ge} + \textit{cis}\text{-}(\mathrm{NO})_2 \rightarrow \mathrm{ONGeNO}, \tag{1}$$

or a further reaction following the formation of GeNO,

$$\mathrm{GeNO} + \mathrm{NO} \rightarrow \mathrm{ONGeNO}. \tag{2}$$

The exothermicity of these two reactions was calculated to be 320 and 110 kJ mol^{-1}, respectively, using the BLYP method. We observed that the lines attributed to both GeNO and ONGeNO increased upon annealing, likewise *cis*-$(NO)_2$. If reaction (1) takes place, one would expect the reaction

$$\mathrm{Ge} + \textit{cis}\text{-}(\mathrm{NO})_2 \rightarrow \textit{cyc}\text{-}\mathrm{GeONNO} \tag{1'}$$

to occur with a greater probability because this path involves the least energy. Hence we think that reaction (2) is a more likely path for the formation of ONGeNO.

Our quantum-chemical calculations indicate that *cyc*-GeONNO readily forms N_2O and GeO via a transition state with a barrier of only ~28 kJ mol^{-1}; the barrier was calcu-

lated by comparison of the energy of the transition state and *cyc*-GeONNO. This mechanism might explain why we observed N_2O and GeO after deposition, but not *cyc*-GeONNO. A similar mechanism is expected to apply for catalytic decomposition of NO dimers to N_2O and GeO. In contrast, Davies and Craig proposed that the NO dimer binds to the Ge surface through its N atoms; subsequent electron bombardment resulted in desorption of N_2O and N_2.[8] Further investigation on this surface reaction is needed.

VII. CONCLUSION

Codeposition of laser-ablated Ge with a mixture of NO in Ar produced new lines in three groups that are assigned to the N–O stretching mode of GeNO (1543.8 cm^{-1} and its overtone at 3059.7 cm^{-1}), the symmetric and antisymmetric N–O stretching modes of ONGeNO (1645.5 and 1482.8 cm^{-1}), and the N–O stretching mode of $GeNO^-$ (1417 cm^{-1}). These assignments were based on the observed and calculated vibrational wave numbers and ^{15}N- and ^{18}O-isotopic shifts, and behaviors upon concentration variation, conditions for photolysis, and annealing. The theoretical calculations also predict that Ge can also react with *cis*-$(NO)_2$ to form *cyc*-GeONNO, followed by decomposition to form N_2O and GeO that were also observed in matrices.

ACKNOWLEDGMENTS

We thank the National Science Council of Taiwan (Grant No. NSC93-2113-M-009-018) for support and the National Center for High-Performance Computing for computer time.

[1] M. L. Green, E. P. Gusev, R. Degraeve, and E. L. Garfunkel, J. Appl. Phys. **90**, 2057 (2001).
[2] K. Fan and S. Iwata, Chem. Phys. Lett. **189**, 401 (1992).
[3] C. Puzzarini, R. Tarroni, P. Palmieri, and S. Cartes, J. Chem. Soc., Faraday Trans. **92**, 4361, (1996).
[4] M. Zhou, L. Jiang, and Q. Xu, J. Phys. Chem. **108**, 9521 (2004).
[5] H. Shang, K.-L. Lee, P. Kozlowski *et al.*, IEEE Electron Device Lett. **25**, 135 (2004).
[6] C. O. Chui, H. Kim, P. C. McIntyre, and K. C. Saraswat, IEEE Electron Device Lett. **25**, 274 (2004).
[7] B. M. Davies and J. H. Craig, Jr., Appl. Surf. Sci. **205**, 22 (2003).
[8] B. M. Davies and J. H. Craig, Jr., Surf. Sci. **529**, 231 (2003).
[9] J. S. Ogden and M. J. Ricks, J. Chem. Phys. **52**, 352 (1970).
[10] A. Bos, J. S. Ogden, and L. Orgee, J. Phys. Chem. **78**, 1763 (1969).
[11] J. S. Anderson, J. S. Ogden, and M. J. Ricks, Chem. Commun. (London) **24**, 1585 (1968).
[12] P. Hassanzadeh and L. Andrews, J. Phys. Chem. **96**, 6181 (1992).
[13] A. Zumbusch and H. Schnöckel, J. Chem. Phys. **108**, 8092 (1998).
[14] M. Friesen, M. Junker, and H. Schnöckel, J. Chem. Phys. **112**, 1782 (2000).
[15] P. C. Marino, J. D. Guerin, and E. R. Nixon, J. Mol. Spectrosc. **51**, 160 (1974).
[16] R. Köppe and H. Schnöckel, J. Mol. Struct. **238**, 429 (1990).
[17] M. Friesen, M. Junker, and H. Schnöckel, Heteroat. Chem. **10**, 658 (1999).
[18] X. F. Wang, L. Andrews, and G. P. Kushto, J. Phys. Chem. A **106**, 5809 (2002).
[19] A. J. Boone, D. H. Magers, and J. Leszczynski, Int. J. Quantum Chem. **70**, 925 (1998).
[20] Z. Palagyi, H. F. Schaefer, and E. Kapuy, J. Am. Chem. Soc. **115**, 6901 (1993).
[21] R. S. Grev, B. J. Deleeuw, and H. F. Schaefer, Chem. Phys. Lett. **165**, 257 (1990).
[22] M. Bahou, K. Sankaran, Y.-J. Wu, Y.-P. Lee, D. Rayner, and B. Simard, J. Chem. Phys. **118**, 9710 (2003).
[23] W.-J. Lo, M.-Y. Shen, C.-H. Yu, and Y.-P. Lee, J. Chem. Phys. **104**, 935 (1996).
[24] M. Bahou, S.-F. Chen, and Y.-P. Lee, J. Phys. Chem. A **104**, 3613 (2000).
[25] A. Noyes, Jr., J. Am. Chem. Soc. **53**, 515 (1931).
[26] M. J. Frisch, G. W. Trucks, H. B. Schlegel *et al.*, GAUSSIAN03 Revision A.1, Gaussian Inc., Pittsburgh, PA, 2003.
[27] A. D. Becke, J. Chem. Phys. **98**, 5648 (1993).
[28] A. Lee, W. Yang, and R. G. Parr, Phys. Rev. B **37**, 785 (1988).
[29] T. H. Dunning, J. Chem. Phys. **90**, 1007 (1989).
[30] L. Krim and N. Lacome, J. Phys. Chem. A **102**, 2289 (1998).
[31] L. Andrews, M. Zhou, S. P. Willson, G. P. Kushto, A. Snis, and I. Panas, J. Chem. Phys. **109**, 177 (1998).
[32] D. E. Milligan and M. E. Jacox, J. Chem. Phys. **55**, 3404 (1971).
[33] See EPAPS Document No. E-JCPSA6-123-018528 for comparison of results from BLYP and B3LYP. This document can reached via a direct link in the online article's HTML reference section or via the EPAPS homepage (http://www.aip.org/pubservs/epaps.html).
[34] C.-I. Lee, Y.-P. Lee, X. Wang, and Q.-Z. Qin, J. Chem. Phys. **109**, 10446 (1998).
[35] K. P. Huber and G. Herzberg, in *NIST Chemistry WebBook*, NIST Standard Reference Database Number 69, edited by P. J. Linstrom and W. G. Mallard (National Institute of Standards and Technology, Gaithersburg, MD, 2003); http://webbook.nist.gov